Publication 5

Dlala, E., Belahcen, A., Arkkio, A., "Efficient magnetodynamic lamination model for two-dimensional field simulation of rotating electrical machines", *J. Magn. Magn. Mater.*, to be published, in press, January 2008.

Journal of Magnetism and Magnetic Materials 00 (2008) 000–000

www.elsevier.com/locate/jmmm

Efficient magnetodynamic lamination model for two-dimensional field simulation of rotating electrical machines

Emad Dlala*, Anouar Belahcen, Antero Arkkio

Department of Electrical Engineering, Helsinki University of Technology, P.O Box 3000, FI-02015 TKK, Espoo, Finland

Elsevier use only: Received date here; revised date here; accepted date here

Abstract

This article presents a 2D-1D time-stepping finite-element model to evaluate the magnetodynamic rotational hysteresis effects in electrical machine laminated cores. The 1D model is at first validated separately and then incorporated into the 2D model using an efficient iterative fixed-point procedure. A viscosity-based hysteresis model is applied in the lamination to account for the dynamic losses while the rotational field quantities are handled by a modified inverted vector hysteresis model. The 2D-1D model is evaluated by computing the core losses of an induction motor and experimental data of the motor are used for verification.

PACS: 75.40.Mg; 75.60.-d; 75.60.Lr.

Keywords: lamination model; iron losses; magnetodynamic vector hysteresis; eddy currents; rotating electrical machines.

1. Introduction

Modeling the characteristics of magnetic materials in electromagnetic field solvers has been commonly limited to the inclusion of simple magnetization curves with single-valued data. This limitation is attributed to the efficiency and simplicity such elementary models often provide as well as the stability of the iterative methods involved in the field solution. Recently, however, quite a few endeavors have been made to integrate advanced models that can adequately characterize the real magnetization behavior. These advanced models commonly employ macroscopic hysteresis models, but rarely consider the eddy currents in the laminations. The eddy current in the lamination is intrinsically a 3D problem but it can be reduced to 2D by using another 1D model for the lamination depth as was proposed by a few researchers [1, 2]. In the latter works, either two separate iterative procedures were applied [1] or reformulation of the problem was introduced [2], rendering the methods more complicated and less efficient. Furthermore, numerical modeling of rotational eddy-current effects together with hysteresis has recently been reported in the literature [3]. There is a rigorous desire among the electrical machine users and designers to consider these effects in the analysis and consequently evaluate the resultant iron losses accurately.

In this paper, two iterative procedures using the fixed-point method are coupled and simultaneously applied in an efficient scheme in which the 1D lamination model is considered to be a nonlinear subproblem in the domain of the 2D model. The 1D model is adequately integrated in the 2D model, and it does not, in principle, exhibit any further computation except for its field solution, which adds to the problem. The fact that the eddy current in the lamination naturally creates a strong nonlinear problem is another independent matter. The locally convergent fixed-point method [4] is applied to the 1D and 2D models, allowing remarkably fast convergence. The rotational field quantities are handled by modifying the inverted vector hysteresis model [5, 6] so that rotational eddy currents are properly modeled. A viscosity-based model is applied in the lamination depth in each direction of the vector model [7].

The lamination model is incorporated and implemented into a 2D finite-element code, which is specifically made for analysis and design of rotating electrical machines. A comparative study with experimental data is conducted.

* Corresponding author. Tel.: +358 94512392; fax: +358 94512991.
E-mail address: emad.dlala@tkk.fi.

2. The 2D-1D Finite-Element Model

The 1D lamination model and the 2D finite-element model are formulated using the fixed-point method (see [4-8] for detailed descriptions of each model). The flowchart of Fig. 1 summarizes the applied equations in which the small letters stand for the 1D quantities and the capital for the 2D. Only the iterative procedures of the field equations are shown in the chart while solving them by the Crank-Nicholson time-stepping scheme is not. The vector field quantities are interfaced by the magnetodynamic vector hysteresis model [6], which is based on the well-known Mayergoyz model. The 1D dynamic model is applied in each direction specified by the vector model. The fixed-point coefficients ν_{1D} and ν_{2D} for the 1D and 2D models, respectively, are calculated efficiently at each time-step using the locally convergent method [4].

The 2D model controls the overall iteration scheme including the stopping criterion because the 2D model plays the main role in modeling the electrical machine. The 1D lamination model can be viewed as the source of nonlinearly of the 2D model, manifesting itself as a nonlinear function. Therefore, the iteration procedure of the two models is conducted in a parallel manner while their solutions are made in series, making the overall scheme highly efficient.

The iteration procedure is carried out in the following steps:

1. Initialize the magnetization-like quantities $\boldsymbol{M}$ and $\boldsymbol{m}$ at the time-step n and the iterate k=0;
2. Put k=k+1;
3. At each iterate k, solve the 2D field for the magnetic vector potential $\boldsymbol{A}$ and subsequently the flux density $\boldsymbol{B}$;
4. Insert the iteration index k and the flux density $\boldsymbol{B}_1$ to the 1D model;
5. If k=1, set the boundary conditions on the surface of the 1D model as $\boldsymbol{a}_1^{s}=2d\boldsymbol{B}_1$, where d is the sheet thickness;
6. For the same iterate k, solve the 1D field for the magnetic vector potential $\boldsymbol{a}$ and subsequently the flux density $\boldsymbol{b}$;
7. Apply the dynamic hysteresis model in the lamination to calculate $\boldsymbol{h}_k$ and $\boldsymbol{m}_k$;
8. Feed back the surface trajectory of the magnetic field strength $\boldsymbol{h}_k^{s}$ to the 2D model, where $\boldsymbol{H}_k=\boldsymbol{h}_k^{s}$;
9. Determine $\boldsymbol{M}_k$ from $\boldsymbol{B}_k$ and $\boldsymbol{H}_k$ and check whether the iteration is convergent or not. If yes, go to the next time-step (step 1) ; if not, go to the next iterate (step 2).

Thus, the nonlinear relation of the 2D model between the magnetic field strength $\boldsymbol{H}$ and the magnetic flux density $\boldsymbol{B}$ is served through the 1D model. The algorithm guarantees that when the 2D model converges, it automatically means that the 1D model has converged, or otherwise the 2D model would not converge. The boundary condition of the 1D model calculated from the 2D model is assumed to remain fixed during the iteration. The 1D and 2D field equations are discretized using first-order finite-elements and solved by the Crank-Nicholson time-stepping scheme.

3. Verifying the Magnetodynamic Hysteresis Vector Model

The magnetodynamic vector hysteresis model has been validated by the 1D lamination model. Experimental data obtained from a modern digital setup, which allows measuring dynamic hysteresis loops in two directions at various flux orientations, have been used to identify the model. The 1D lamination model used for the validation of the magnetodynamic vector hysteresis model is the same model described in the previous section (see Fig. 1), except that in this case the 1D model is not integrated into the 2D model. The averaged values of the flux density $\boldsymbol{B}$ are now imposed from the measured flux waveforms. The calculated quantity $\boldsymbol{H}=\boldsymbol{h}^{s}$ on the surface is used as the output of the model.

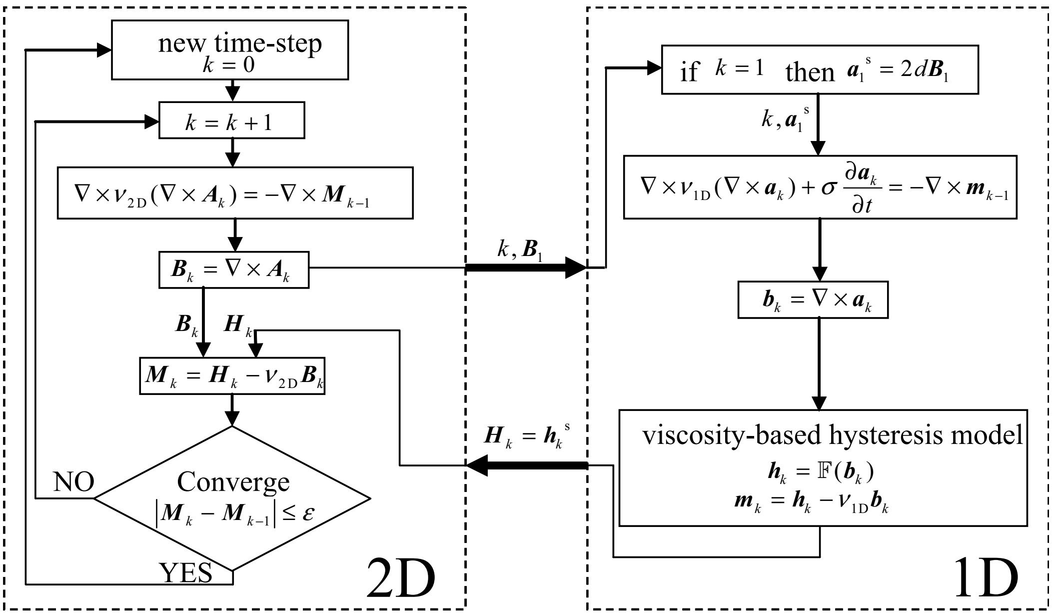

Fig. 1. Flowchart of the 2D-1D model.

The identification method of the magnetodynamic vector hysteresis model has been described in [6]. Unlike the identification process of the vector hysteresis model [9], which is difficult and may lead to rather tedious calculations, identifying model [6] is simple and straightforward. In principle, only a few parameters need to be identified to best fit the simulated dynamic loops to the measured ones. Fig. 2 illustrates dynamic loops measured under elliptic excitation at 50 Hz in the *x*- and *y*-directions and compared with the modeled ones.

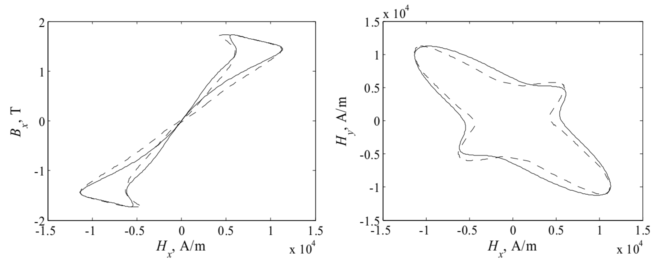

Fig. 2. The 1D model prediction (dotted) verified by experimental data (solid).

It is observed that the vector hysteresis model gives rather reasonable results in general. The four rising convex shapes in the loci of the magnetic field strength (which also appear in the rising wings in the *B-H* loop) occurred in the measurement because only four coils, and four sensors, vertically placed, were used in the measuring setup. This phenomenon is commonly occurring in most of the 2D measuring setups [10], but yet has not been well reported. In the modeling stage, the convex shapes in the loci of the magnetic field strength are achieved by using the generalized Mayergoyz model [11], which coincidentally, it should be said, exhibits the same behavior of the measurement. Such a study on the phenomenon is currently being conducted [12].

4. Simulation of Induction Motor

The 2D-1D finite-element model developed in this work has been applied to predict iron losses in a 400-V, 50-Hz, 4-pole, 37-kW squirrel-cage induction motor. The core losses of the motor were measured at no load with various voltage levels and they have been segregated from the total electromagnetic loss using a rigorous method [13]. The method enforces the motor to run at the synchronous speed ensuring that no friction or windage mechanical losses are apparent in the measurements. Furthermore, the method suppresses the negative torque caused by the harmonics. The iron losses are then separated from the total electromagnetic losses by subtracting the resistive loss of the stator. The result of the subtraction can be assumed to be purely associated with the core losses.

The induction motor is in general considered to be one of the most difficult nonlinear problems, especially when its stator and rotor are slotted. The slotting of the motor causes significant problems to the time-stepping scheme, and thus to the iterative procedures because of the high harmonics induced.

For a comparison purpose, the same 2D time-stepping finite-element model without the 1D model has been applied to predict the core losses using a single-valued magnetization curve. Although the iron losses in the single-valued model are not considered in the field solution and their effect cannot be evaluated, such a model is the most common numerical tool available nowadays in commercial and research software to predict core losses in electrical machines. The iron losses are calculated from the statistical loss law using a post-processing Fourier analysis of the field solution.

To avoid modeling the transient of the motor starting, a time-harmonic model was applied to calculate the initial values of the steady-state solution before the time-stepping model has been used. Then, the time-stepping analysis using the 2D-1D model or the 2D single-valued model is run over several periods T of the supply voltage to ensure that the steady state is reached. (5 periods were used in our simulation with 600 time-steps per period.) In the case of the 2D-1D model, the total iron losses in the machine are computed from the Poynting vector using the following integral:

$$p_{\mathrm{c}} = \frac{1}{T}\int_T \boldsymbol{H}.\frac{\mathrm{d}\boldsymbol{B}}{\mathrm{d}t}\mathrm{d}t = \frac{1}{T}\int_T \left(H_x.\frac{\mathrm{d}B_x}{\mathrm{d}t} + H_y.\frac{\mathrm{d}B_y}{\mathrm{d}t} \right)\mathrm{d}t \quad (1)$$

The total iron losses are separated into two components according to Atallah's theory [14]. The first one is resulted from the effect of the flux rotation and the second from the flux alternation. Furthermore, the magnetodynamic effects are separated into hysteresis, excess, and eddy-current losses according to the systematic method proposed in [15]. The viscosity-based model automatically allows for the separation of the iron losses.

5. Results

This section presents the numerical results of the iron losses obtained by implementing the finite-element procedures described above. Fig. 3 shows the calculated total iron losses by the 2D-1D model compared with the measured iron losses obtained from the synchronous no-load test. The small discrepancies between the measured and modeled results could be associated with the harmonics. The negative-torque harmonics induced in the iron and copper of the rotor are modeled in the field solution; thus, their effect is evaluated in the computation (but not in the measurements). The single-valued model gives relatively acceptable results at lower level of voltages (lower flux densities) but becomes remarkably inaccurate at higher induction.

The stator core losses are separated as shown in Fig. 4. It is observed that, although the voltage increases in the stator, the static hysteresis losses decrease because at saturation the rotational losses drop. The hysteresis loss is predominant in the motor stator. However, the eddy-current losses are predominant in the rotor core (see Fig. 5) and they sharply increase with the increase of the supply voltage. The high-harmonics resulted from slotting have a direct influence on the eddy-current losses. In Fig. 6, the total core losses of the motor are separated into alternating and rotating components.

The rotational loss component contributes by ~30% of the total core losses at the rated voltage.

The dynamic *B-H* loops and their loci at a point in the stator yoke where the flux is noticeably rotational are plotted in Fig. 7. The sum of the area of the *B-H* loops in the *x*- and *y*-directions represents the core losses dissipated at that point.

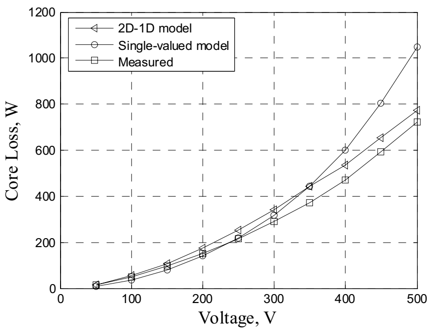

Fig.3. Total core losses of the 37-kW induction motor.

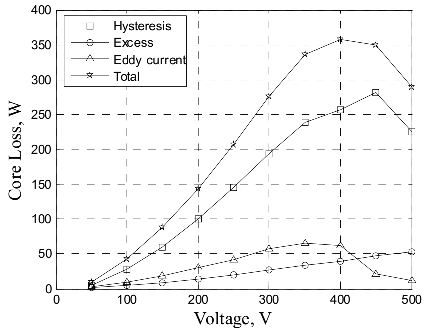

Fig.4. Separation of the stator core losses computed by the 2D-1D model.

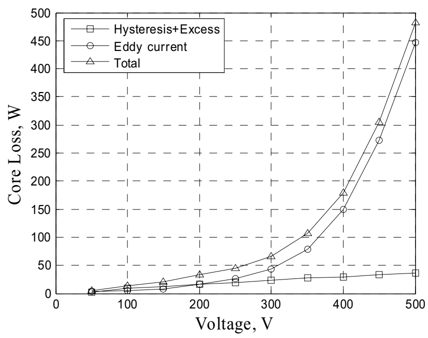

Fig.5. Separation of the rotor core losses computed by the 2D-1D model.

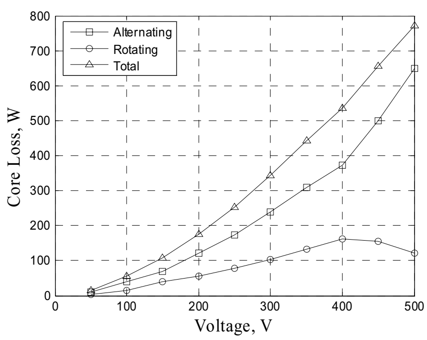

Fig.6. Separation of the motor core losses computed by the 2D-1D model.

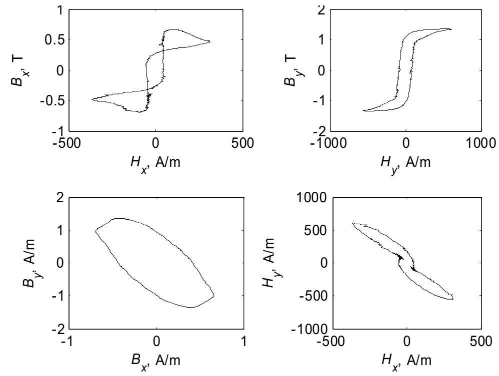

Fig.7. Dynamic *B-H* loops and their loci at a point in the stator yoke.

6. Conclusions

This article proposed a new technique for calculating the magnetodynamic iron losses in electrical machine laminated cores. The proposed 2D-1D model has been applied to predict iron losses in an induction motor. The comparison of the computed and measured data reveals that the model is fruitful and can be used for design purposes. Although the 2D-1D model is efficient comparing with its peers, for example 3D modeling, integrating the 1D model into the 2D model increases the overall computation time rather significantly. The number of iterates increases because of the strong eddy-current nonlinear problem. Furthermore, the solution of the 1D model adds to the computation time at each iterate and for each direction of the vector hysteresis model. Further improvement and study regarding the model is the goal of future work.

References

[1] O. Bottauscio, M. Chiampi, D. Chiarabaglio, IEEE Trans. Magn., 36 (2000) 573.
[2] O. Bottauscio, M. Chiampi, IEEE Trans. Magn., 38 (2002) 2358.
[3] O. Bottauscio, M. Chiampi, J. Appl. Phys., 89 (2001) 6728.
[4] E. Dlala, A. Belahcen, A. Arkkio, IEEE Trans. Magn., 43 (2007) 3969.
[5] E. Dlala, J. Saitz, A. Arkkio, IEEE Trans. Magn., 42 (2006) 1963.
[6] E. Dlala, A. Belahcen, A. Arkkio, Physica B, 403 (2008) 428.
[7] S. Zirka, I. Moroz, P. Marketos, A. Moses, IEEE Trans. Magn., , 42 (2006) 2121.
[8] A. Arkkio, Acta Polytechnica Scandinavica, 59 (1987).
[9] I. Mayergoyz, New York, Springer-Verlag, (1991).
[10] W. Brix, K. Hrmpel, F. Schult, IEEE Trans. Magn., 18 (1984) 1708.
[11] A. Adly and I. Mayergoyz, J. Appl. Phys., 73 (1993) 5824.
[12] E. Dlala, submitted to Intermag 2008, Madrid.
[13] E. Dlala, A. Arkkio, IET Proc., Electr. Power Appl., 1 (2007) 737.
[15] K. Atallah, D. Howe, IEEE Trans. Magn., 29 (1993) 3547.
[16] S. Zirka, I. Moroz, P. Marketos, A. Moses, IEEE Trans. Magn., 41 (2005) 1109.